ORIGINAL PAPER

Photocatalytic Degradation of Eriochrome Black T Dye by ZnO Nanoparticles Using Multivariate Factorial, Kinetics and Isotherm Models

Muhammad Farooque Lanjwani[1,2] · Muhammad Yar Khuhawar[3] · Taj Muhammad Jahangir Khuhawar[3] · Abdul Hameed Lanjwani[4] · Saima Qayoom Memon[1] · Waheed Ali Soomro[3] · Imran Khan Rind[5]

Abstract

In current study the photocatalyst ZnO was prepared by complexation of zinc acetate with sodium diethyl dithiocarbamate trihydrate, and calcined at 750 °C. The ZnO nanoparticles were characterized by DLS, Zeta potential, SEM, EDX and FTIR. The ZnO nanoparticles (NPs) were applied for photocatalytic degradation of Eriochrome black-T (EBT) dye by UV, visible and mercury light irradiation sources. The experimental conditions were optimized by univariate and multivariate techniques, and it was revealed that degradation of dye by ZnO NPs surface was dependent on source of light and pH of dye solution. The degradation of EBT dye at pH 11 showed highest degradation rate 99.64% with UV light. The ZnO was calcined at 450, 600, 750 and 900 °C, but the calcination temperature 750 °C showed better degradation rate for EBT. The highest degradation was found at 15 mg dose and 5 ppm concentration. The effects of Na^+, Ca^{2+}, K^+, Mg^{2+} on the degradation, were studied and these salts had no effect on degradation rate. The degradation obeyed pseudo second order kinetics model as compared to pseudo first and zero order models and Langmuir isotherm model fitted more as compare to other models. The effects of variables were examined by factorial design of 18 experiments by cantered Draper-Lin small composite model. The degradation of EBT dye in real samples collected from River Indus, tape water and domestic wastewater and spiked with 20 µg/mL, indicated that the dye degraded upto 82–86% with relative standard deviations (RSD) within 2% (n = 3).

Keywords ZnO · Eriochrome black T · Photocatalytic degradation · UV irradiation · Sample analyses · Effect of variables

✉ Muhammad Farooque Lanjwani
farooque.lanjwani@scholars.usindh.edu.pk

Muhammad Yar Khuhawar
mykhuhawar@usindh.edu.pk

Taj Muhammad Jahangir Khuhawar
tmj.iarscs@usindh.edu.pk

Abdul Hameed Lanjwani
ahlanjwani@smbbmu.edu.pk

Saima Qayoom Memon
saimaqmemon@usindh.edu.pk

Waheed Ali Soomro
waheedsomro88@yahoo.com

Imran Khan Rind
irind87@gmail.com

[1] Dr M. A. Kazi Institute of Chemistry, University of Sindh, Jamshoro, Sindh, Pakistan

[2] Chemistry Department, Faculty of Science and Arts, Tokat Gaziosmanpasa University, 60250 Tokat, Turkey

[3] Institute of Advanced Research Studies in Chemical Science, University of Sindh, Jamshoro, Pakistan

[4] Shaheed Mohtarma Benazir Bhutto Medical University, Larkana, Sindh, Pakistan

[5] National Centre of Excellence in Analytical Chemistry, University of Sindh, Jamshoro, Sindh, Pakistan

Introduction

During last a few decades, the fast growth of industrialization has caused overdoing of textile dyes, pesticides, antibiotics and fertilizers and these pollutants are discharged in the environment. These pollutants have carried great risk to human life and ecosystems by bioaccumulation, ecotoxicological effects and antibiotic resistance [1, 2]. Organic dyes are colored and durable compounds and are extensively utilized in industrial manufacture of dying agents, textile, leather, paint, clothing, rubber, biological imaging, plastic paper making and food processes etc. Though, due to the utilizing a large volume of organic dyes are causing damage to human lungs, kidneys, organs and carcinogenic effects. The most common organic dyes are EBT, MO, MG, Congo red (CR), MB, and so on [3, 4]. Under the background of environment deterioration and energy crisis, photocatalysis is most inspired and effective approach for the conversion of solar-chemical energy in green-chemical fields such as photodegradation of organic contaminants. The photocatalysis procedure comprises two chief aspects, migration and separation of photo-electrons and the holes under irradiation, and interaction among reactants and active component. The most critical issue in the photocatalysis is to enable the active component to contribute in photochemical reaction under the evidence of maximum contact active positions and adsorption reactants [5]. Photocatalysis is expediently being used for the degradation of dyes pollutants into CO_2, H_2O, colorless products and minerals without producing any secondary pollutant. Metal oxide semiconductor nanomaterials, like ZnO [6], TiO_2 [7], Fe_2O_3 [8], CdS [9], and ZnS [10], are applied as a photocatalyst. These are effective, environment-friendly and cost-efficient materials and may be applied to improve environmental difficulties. It is described that amongst many semiconductors, zinc oxide (ZnO) shows good competence in the degradation of many dyes, as compared to titanium oxide (TiO_2) as photocatalyst, because ZnO is low cost with high catalytic efficiency, nontoxic in nature with large band gap (3.37 eV) [11–13]. The effect of many parameters like UV light intensity, pH of the medium, amount of photocatalyst, initial concentration of dye [14, 15] and doping have been reported [16]. The morphology of zinc oxide (ZnO) nanoparticles can be manipulated by modifying the reaction parameters including the temperature, pH, concentration of solution, complexing agent and heating duration. Different morphologies of ZnO particles like nanoprisms [17], nanorods [18], nanoflowers [19], nanosheets [20] and nanodisks [21] have been synthesized and reported. Eriochrome Black T (EBT) is most significant azo dyes that is used in dyeing wool, silk, multifibres, nylon, and is also used for estimations of Mg^{2+}, Ca^{2+}, and Zn^{2+} by complexometric titrations.. The EBT is harmful dye even if it is present as a middle product naphthaquinone and is carcinogenic. Hence, EBT dye is a serious concern around the whole globe for its active treatment from wastewater [22]. The main objective of the current research work was to prepare zinc oxide (ZnO) nanoparticle by chemical precipitation using complexation method and apply for the degradation of EBT dye under optimized conditions. The work also examined the degradation of EBT from real samples.

Materials and Methods

Chemical and Reagents

Zinc acetate and sodium diethyldithiocarbamate were purchased from Merck, Darmstadt, Germany. All chemicals applied were of reagent or analytical grade.

Preparation of ZnO Nanoparticle

For the preparation of ZnO NPs, 2.74 g of zinc acetate dihydrate ($Zn(CH_3CO_2)_2 \cdot 2H_2O$) was dissolved in 250 ml deionised water to prepare (0.05 M) (solution A). 5.63 g of sodium diethyldithiocarbamate trihydrate dissolved in deionized water (500 mL) (0.1 M) (solution B). The solution B was added dropwise into zinc acetate solution A at constant stirring and then mixture was continuously stirred for two hour. The white precipitate obtained was centrifuged for 15 min at 3500 rpm and washed several time with deionized water. The zinc complex of diethylditiocarbamate was initially prepared as reported following general procedure [23]. The white precipitate was dried at 70 °C for 24 h. Finally, ZnO NPs were obtained by calcination of the precipitate at different temperatures 450, 600, 750 and 900 °C in muffle furnace.

Characterisation of ZnO Nanoparticles (NPs)

The ultraviolet and visible spectra of ZnO NPs were examined by double-beam spectrophotometer (Hitachi 220 (Pvt) Ltd, Tokyo, Japan) using dual 1 cm silica cuvettes. The FT-IR spectra of ZnO nanoparticles (NPs) were noted on FT-IR (Thermo Scientifc™ Nicolet™ iS10) spectrometer through Attenuated total reflectance (ATR) accessory and spectra were noted within 4000–600 cm^{-1} using OMNIC™ Software. The morphology and elemental composition of ZnO (NPs) were noted using SEM and EDX (JEOL JSM-6490 LV) instrument at Center for Pure and Applied Geology, University of Sindh, Jamshoro. The DLS and zeta potential of ZnO NPs were measured using Zeta sizer Nano-ZS Malvern Inc, London UK from Department of

Metallurgy and Materials Engineering, Mehran University of Engineering and Technology, Jamshoro.

Preparation of Eriochrome Black T Dye Solution

EBT dye (0.10 g) was dissolved in 100 ml deionized water to prepare 1 mg/mL (1000 ppm) solution. Further solution were prepared from stock by appropriate dilution by deionized water. The structural formula of EBT dye is shown in (Figure S1). The dye wastewater sample was also collected from (Archroma company limited Jamshoro) and used for photodegradation without any purification.

Photocatalytic Activity

The photocatalytic efficiency of ZnO NPs were assessed with a degradation of EBT using UV fluorescent light irradiation (Black light, compact fluorescent, made in China) 40-W lamp with wavelength 365-nm, mercury lamp (Leo Star) 160 W and visible light 100 W (Jeyo, blub). In a representative process, 10 mg of ZnO NPs were added to 50 mL of solution containing 20 μg/mL EBT dye concentration and pH was adjusted to 11. Then, solution was kept in the dark for 10 min and was stirred. The solution was irradiated for 30 min. The space between lamp and reactor was 10 cm and dye reaction solution was stirred continuously. The 5 mL of EBT dye sample was taken at 10 min interval and instantly centrifuged at 5000 rpm for 5 min to isolate the photocatalyst particles. Finally, absorbance of dye sample was noted at UV Visible spectrophotometer (Hitachi model 220) at 545 nm wavelength. The degradation rate (η) of EBT dye was calculated as below:

$$\eta = C_0 - C_t/C_0 \times 100$$

where C_0 indicates initial concentration of EBT dye and C_t stand for final concentration of dyes at different irradiation times.

Kinetics Models

The kinetic models pseudo zero order, first and second order were applied to describe the degradation process of EBT dye. These models were calculated as below:

$$r = -dC/dt = k_{photo\,0}\,C$$

$$r = -dC/dt = k_{photo\,1}\,C$$

$$r = -dC/dt = k_{photo\,2}\,C$$

where r express the rate of EBT degradation (mol L^{-1} min^{-1}), C express the concentration at given time interval (mol L^{-1}), kphoto, 0 is zero order rate constant (mol L^{-1} min^{-1}), $k_{photo,1}$ is the first-order rate constant (min^{-1}), and $k_{photo,2}$ is the second-order rate constant (L mol^{-1} min^{-1}) [24].

The non-linearized equation of zero, first, and second-order kinetics were calculated by following equations.

$$C = C_0 - k_{photo;\,0}\,t$$

$$C = C_0 - k_{photo;\,1}\,t$$

$$C = C_0 - k_{photo;\,2}\,t$$

where C_0 showed initial concentration dye solution. Nonlinear regression was applied to evaluate the parameters used in the zero, first and second-order kinetics expressions [24].

Isotherm Models

Langmuir linear isotherm model was used to examine the maximum degradation amount of EBT dye and it was calculated by below equation:

$$Ce/qe = 1/Q_o b + Ce/Q_o$$

where qe is degradation quantity at equilibrium in mg/g, Ce stand for initial concentration of EBT dye, Q_0 is maximum degradation capacity and b denotes Langmuir equilibrium constant as mL/mg.

The modified Freundlich model describes obtained data in expressions of diffusion-controlled and ion exchange process. A Freundlich model shows a heterogeneous surface binding.

$$Log = \left(1 - C/C_0\right) = \log k + b \log t$$

The C_0 and C represent the concentration of dye in solution at time 0 and t, respectively, k indicates rate constant, where b constants whose chemical importance is not clearly determined [25].

Design of Experiments for Optimization

The factorial design was applied to examine the important variables and their values. It is a design by which interaction between all parameters may be examined. The present work examined factorial design of 18 experiments by centered Draper-Lin small composite model. The independent levels of variables, were three coded levels such as − 1, 0 and + 1 for low, medium and high values of individual variables used for design the experiments (Table 1) and examine the interactive effects of variables such as pH, concentration of dye, catalyst dose and degradation time [26, 27]. In the present study multi-variant method was applied

Table 1 Experimental design for photocatalytic degradation of EBT dye by the ZnO nanoparticles

Trial	Coded values			
	A	B	C	D
1	− 1	+ 1	− 1	+ 1
2	+ 1	− 1	+ 1	+ 1
3	− 1	− 1	− 1	− 1
4	0	− 1	0	0
5	− 1	− 1	+ 1	− 1
6	+ 1	0	0	0
7	+ 1	− 1	− 1	+ 1
8	+ 1	+ 1	+ 1	− 1
9	0	0	− 1	0
10	− 1	+ 1	+ 1	+ 1
11	+ 1	+ 1	− 1	− 1
12	0	+ 1	0	0
13	− 1	0	0	0
14	0	0	0	+ 1
15	0	0	0	− 1
16	0	0	+ 1	0
17	0	0	0	0
18	0	0	0	0

Table 2 Levels of factors used in experimental design for the photocatalytic degradation of EBT dye by the ZnO nanoparticles

Independent variables	Coded levels		
	− 1	0	+ 1
pH, A	4	7	11
Concentration (mg/L), B	5	15	25
Amount (mg), C	5	15	25
Time, (min), D	10	20	30

for optimization of parameters to examine the interactive effects of parameters. For the experimental design four variable were taken within the range, pH 4–11, dye concentration 5–25 μg/mL, catalyst dose 5–25 mg/50 mL and time 10–30 min for each trail (Table 2).

Results and Discussion

The zinc complex of diethylditiocarbamate was initially prepared as reported following general procedure [23]. The colourless precipitates obtained were separated by centrifugation. The dried precipitates were then heated in furnace at different temperatures. The obtained ZnO NPs were then characterized using different techniques.

Characterization of Synthesized ZnO Nanoparticles

Scanning Electron Microscopy (SEM)

The SEM is a useful technique for the higher resolution of surface imaging to know the nanostructures at microscopic level that uses electron beam for the surface imaging. Larger field depth and higher magnification makes SEM images beneficial to know surface topological information of several nano particles and depends on electron density of surface [28]. The four different SEM images were analyzed 100 μm, 50 μm, 20 μm and 10 μm (Fig. 1). The SEM images clearly showed the existence of synthesized ZnO nanoparticles. The nanoparticles were spherical, oval in shape, aggregated porous powder like morphology and some individual particles were also observed. The agglomeration could be convinced by densification resulting of narrow space among the particles. The SEM image showed mostly particles of ZnO NPs were in small size but some particles appeared with higher particle sizes also. The figure b showed cloud point structure. The figure c and d particle size were achieved at higher zoom 20 and 10 μm.

Dynamic Light Scattering (DLS) Analysis

The distribution of particle size was analyzed by DLS technique. The DLS is an instruments generally used for the measuring of the particle size of disperse solution to analyze the thickness of nanoparticles with the real size of the metal nanoparticles [29]. The DLS results showed one peak 100% particles size of 88.1 nm (Fig. 2). Therefore results indicated that most of particles size were less than 100 nm.

Zeta Potential (ZP) Analysis

Zeta potential (ZP) measurement was carried out to know the surface charge and also stability of zinc oxide nanoparticles (ZnO NPs) [30]. The zeta potential average results showed − 31.45 mV, peak one showed − 21.40 mV in 95.0% and peak two showed − 62.71 mV in 5.0% (Fig. 3). The zeta potential results revealed that ZnO nano particle indicated good potential.

FTIR

FTIR spectroscopy is a great technique used for the characterization and identification of materials and compounds by examining their unique modes of vibration [28]. The two spectra of FTIR of ZnO NPs were obtained before calcination and after calcination. The spectrum before calcination showed a number of peaks, due to the complexing reagent used for preparation of ZnO NPs. The peaks at 2900 cm^{-1} showed C–H stretching, peak at 1500 cm^{-1} indicated C=N,

Fig. 1 SEM images of ZnO nanoparticle **a** 100 μm, **b** 50 μm, **c** 20 μm and **d** 10 μm
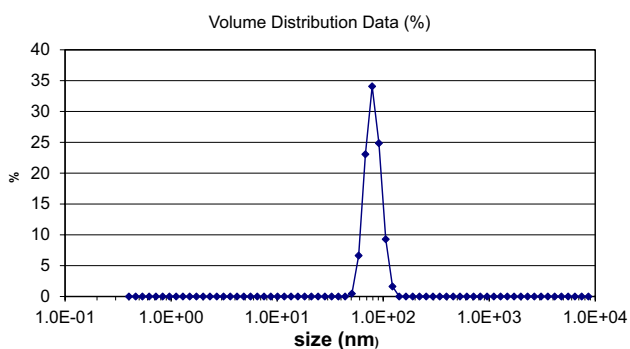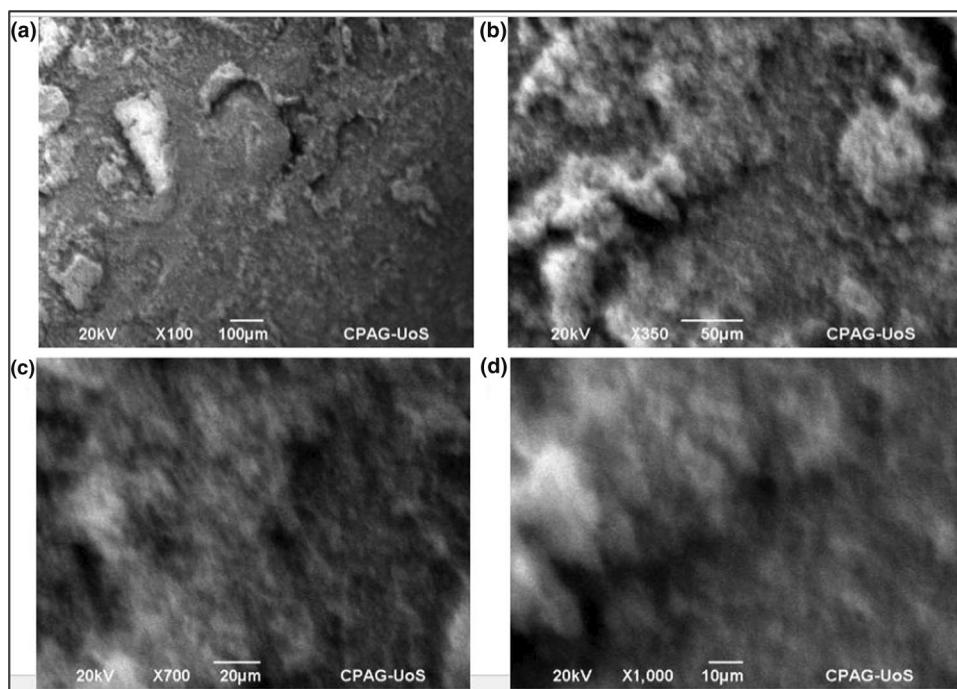

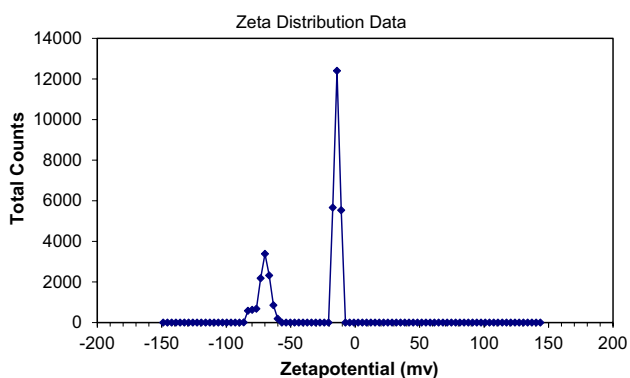**Fig. 2** Dynamic light scattering (DLS) analysis of ZnO

Fig. 3 Zeta potential analysis of ZnO

peak at 1447 cm^{-1} indicated CH2, at 1377 cm^{-1} for CH3, and at 1072 cm^{-1} for C=S groups (Fig. 4a). The ZnO NPs after calcination showed peak at 666 cm^{-1} revealed the metal oxide in the NPs (Fig. 4b).

Energy Dispersive X-Ray (EDX)

The EDX is a powerful technique used for the find out the elemental composition of the nanoparticles or any other materials. The EDX of prepared ZnO was examined and the assigned peaks were for Zn and O, without any contamination peaks. The percentages by weight of Zn and O were 77.92% and 22.08%, respectively (Fig. 5). The result confirm that synthesized ZnO nanoparticles were was pure and no other element present in the prepared nanoparticles.

Photocatalytic Activity

Photocatalytic Activity of ZnO for the degradation of EBT dye was examined. The effects of the concentration of dye, dose of photocatalyst, pH, calcination temperature, time of irritation, different light source and effect of interfering ions were investigated.

Among the several approaches, photocatalysis is very effective approach which is producing clean energy (H$_2$), fix ecological problems, and most significantly, all these conversions are driven through infinite solar energy. The power of solar light is about 100 mW/cm^2 (10^7 photons per square centimeter), means that there are around 100 photons to arrive at one atom in one second. The absorption
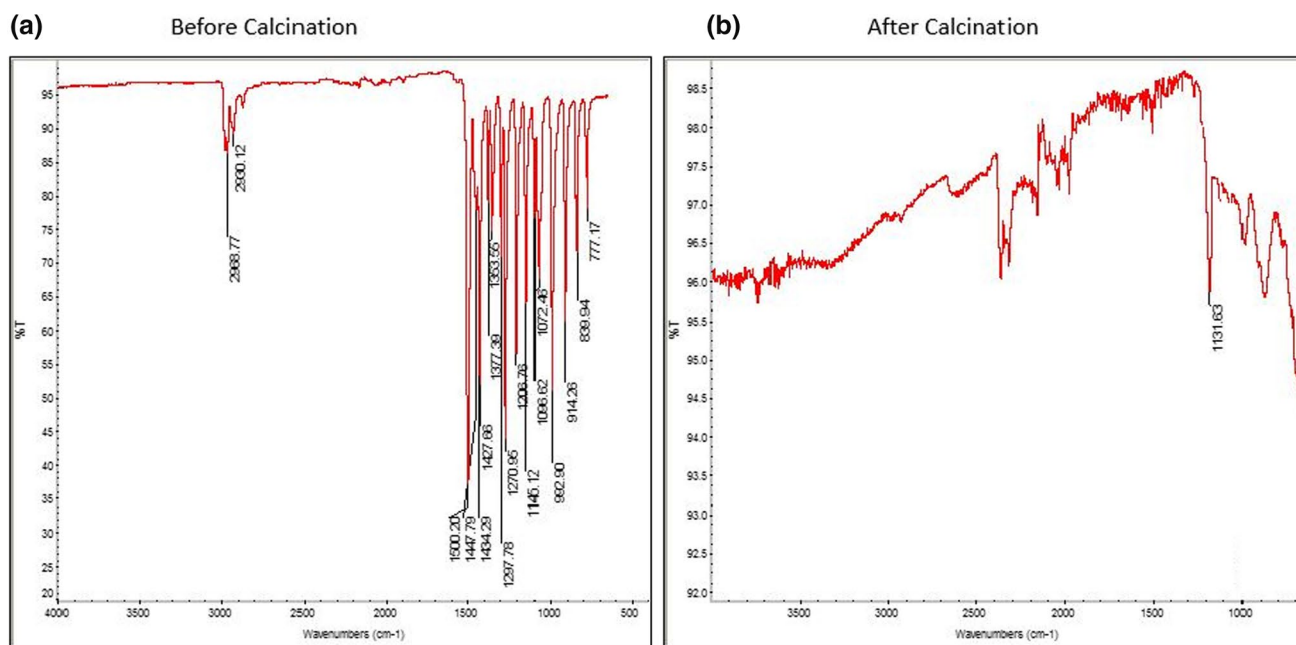
(a) Before Calcination

(b) After Calcination

Fig. 4 FTIR before calcination (**a**) and after calcination (**b**) spectrum of ZnO nanoparticles
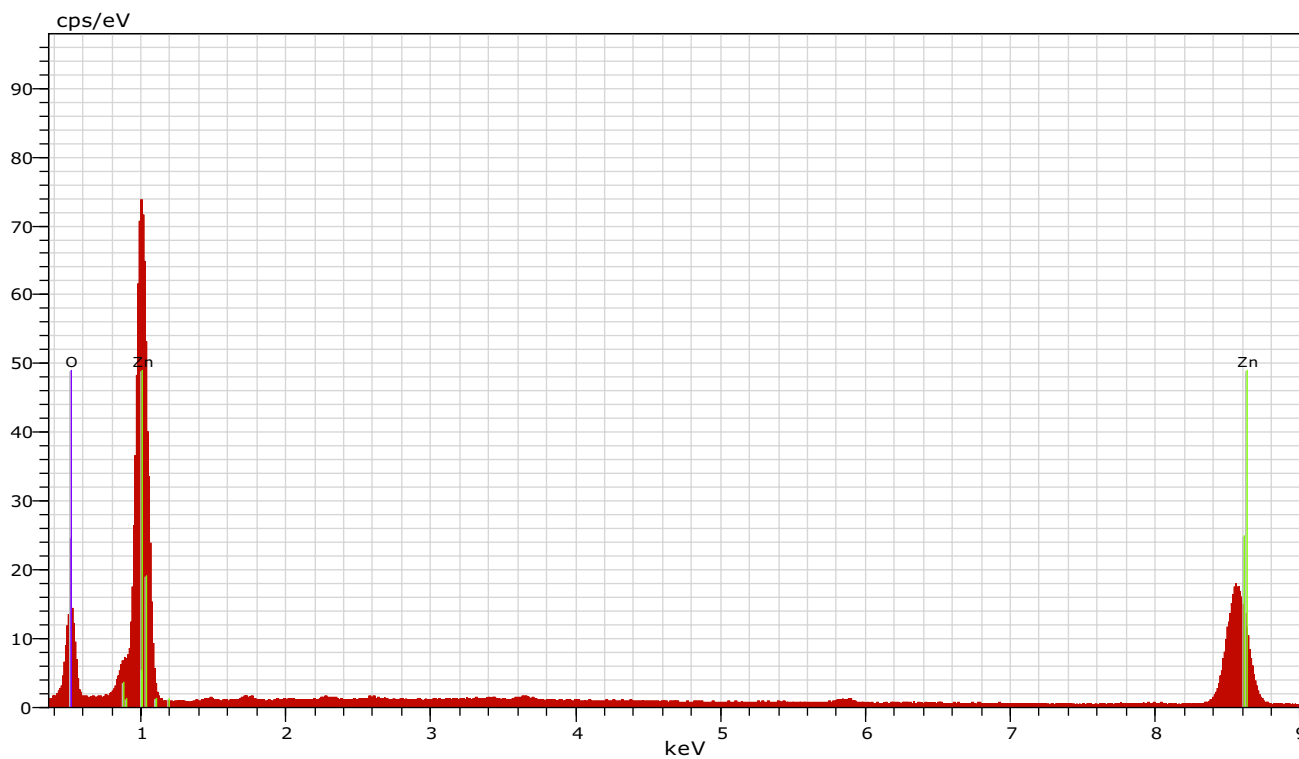

Fig. 5 Energy Dispersive X-Ray analysis of ZnO nanoparticles

of semiconductor photocatalyst materials being generally in the ultraviolet region. Hence, it is interest to find ways to increase the absorption ability in wavelength range as

well as improving the absorption strength. There are several strategies developed to make efficient photocatalyst, like doping, size modulation, band gap engineering, morphology

and loading by metal and non-metals [31]. For better understanding the photocatalysis processes, the measurement of intermediate products is very crucial to assess the degradation way. Though, the real-time study of intermediate yields during the experiment is still quite difficult. The half-life of many intermediate product is short and challenging to be detected, and many intermediate products are not easily recognized using many analytical instruments and methods. Simultaneously many types of intermediate species existing and it is impossible to be identified quantitatively by real-time analytical methods and instruments. Most reported works mostly focus on the assessment of the comparative contribution of active species for degradation of organic impurities. The mechanism of degradation is assumed from qualitative analysis of active species by adding of different scavengers. Until no any report is available for quantitative examination of intermediate yields in photo-degradation processes [32].

Initial Concentration (ppm)

The initial concentration of Eriochrome black T (EBT) dye was changed from 5 to 30 ppm at an interval of 5 ppm. The photocatalytic degradation of EBT dye was examined for 30 min at optimized conditions (Figure S2). The photocatalytic degradation of EBT decreased from 99.73%, 99.64%, 99.11%, 98.43%, 90.72% and 84.21%, at 5, 10, 15, 20, 25 and 30 µg/mL respectively. Therefore, photocatalytic degradation effectiveness of EBT was greater at the lower concentration of dye and was acceptable upto 20 µg/mL. This may be described that more and more molecules of dye were degraded on the surface of the ZnO photocatalyst at lower concentrations than at higher concentrations. Moreover, photons were blocked before reaching in the photocatalyst surface at higher concentrations, therefore, the degradation by photons were reduced and use of 20 ppm concentration of the dye was examined.

Dosage of ZnO

The photocatalytic degradation rate of the EBT dye (20 µg/mL) was examined with ZnO photocatalyst (10–30 mg/50 mL). The photocatalytic degradation efficiency of EBT was 80.35%, 99.32%, 99.65%, 99.83%, 91.26%, and 84.57% at 5, 10, 15, 20, 25 and 30 mg/50 mL of ZnO respectively (Figure S3). When photocatalyst ZnO amount was increased, more active sites were achieved on photocatalyst surface up to certain concentrations with the increase in the formation of radicals. However, further higher dosages of ZnO did not increase the degradation rate of EBT dye. Therefore, 10 mg of ZnO dose was selected for further study [33, 34].

Initial pH of Solution

The pH of dye solution is a main factor in degradation processes. The pH of solution was adjusted with NaOH and HCl (0.1 N). The photocatalytic degradation rates of EBT dye on ZnO were 68.79%, 77.88%, 80.94%, 90.28%, 97.95%, 95.30% and 86.21% at pH levels of 4.0, 6.0, 8.0, 10.0, 11, 12 and 13 respectively (Figure S4). The photocatalytic degradation was higher when initial pH level of dye solution was basic. But was low at acidic pH levels. The highest photocatalytic degradation of EBT dye was found at 11 pH. This phenomenon might be recognized to the compositions of Eriochrome black T dye and photocatalyst surface-charge properties. At acidic pH level, the low photocatalytic degradation rate of dye was achieved due to negligible electrostatic attraction among dye owing to protonations of anions and positively charged photocatalyst surface, resulting in decrease the degree of photocatalytic degradation. But at high pH, high electrostatic attraction occurred among dye anions and photocatalyst surface, resulting in high photocatalytic degradation of dye. The point of zero charge (PZC) of zinc oxide (ZnO) is around pH 9 [35]. The ZnO at pH < PPZC, surface of ZnO is positively charged (at acidic pH level) which reduces the active sites existing for degradation or adsorption of the cationic dye such as EBT. At pH > Pzpc, the surface of ZnO is negatively charged (at basic pH 10). Hence at the basic pH, the hydroxyl group on surface at ZnO is raised which facilitates degradation of EBT dye as well as its self degradation [36].

Calcination Temperature Study

The ZnO photocatalyst was prepared at different calcination temperatures (450, 600, 750 and 900 °C) to compare of the activities of ZnO NPs. The self degradation blank test of EBT was also noted. The degradation rate of EBT was very low in blank condition and was 3.12%. The degradation rate of EBT over ZnO initially increased upto 750 °C, then reduced with rise in the calcination temperature up to 900 °C. The degradation of different calcination of 450 °C, 600 °C, 750 °C, 900 °C were 94.09%, 95.76%, 99.83% and 74.40% respectively (Figure S5). The degradation rate of the ZnO versus EBT dye followed order 750 °C > 600 °C > 450 °C > 900 °C after irradiation of UV light for 30 min, which may be associated to the photocatalyst ZnO particle size.

Comparison of Different Light Sources

The photocatalytic activity of ZnO was assessed through photoreaction method using degradation of EBT dye with the help of fluorescent black light, for UV irradiation using wavelength 365-nm, mercury lamp 160 W and visible light 100 W. The 10 mg of photocatalyst ZnO was added to 50 mL

dye solution with a concentration of 20 µg/mL. The photocatalytic degradation of dye with fluorescent black light was 99.24%, mercury 94.02 and with visible 46.89% (Figure S6). The results showed that fluorescent black light degradation rate was faster than mercury and visible light.

Time Study

At the optimized conditions with the concentration of dye 15 µg/mL, the effect of time was observed from 10 to 50 min. The highest photocatalytic activity was achieved upto 30 min, and after that no significant degradation was achieved. The degradation was observed from 79.58, 90.84, 99.23, 99.24 and 99.23% at 10, 20, 30, 40 and 50 min respectively (Figure S7). Therefore 30 min time was selected for degradation.

Effect of Parameters on the Photocatalytic Activity of EBT Dye

Interference Study

The essential salt were used to check their interference on photocatalytic degradation of EBT dye. The 1000 µg/mL (1 mL) of Na^+, K^+, Ca^{2+}, Mg^{2+}, Cl^- and SO_4^{2-} were added to 50 mL of the solution and then solutions were used for degradation at optimized conditions. The degradations observed were with Ca^{2+} 99.06%, Na^+ 98.00%, Mg^{2+} 97.76%, K^+ 96.96%, Cl 98.20% and SO_4 97.80% (Figure S8). The degradations were in order $Ca^{2+} > Na^+ > Mg^{2+} > K^+$. The interference study showed that the salts did not interference in the photocatalytic degradation rate.

Photodegradation of Dyes Wastewater

The real dye wastewater samples were also collected and checked their photodegradation. The real dye wastewater sample was collected from (Archroma company limited Jamshoro) and used for photodegradation without any purification. The highest photodegradation was obtained on fluorescent light 71.08%, mercury lamp 65.12% and visible light 27.26%. The results revealed the dyes wastewater effected the degradation because dye wastewater contained complex mixture of many dyes which reduced the degradation efficiency.

Spiked Real Sample Analyses

The three samples were collected from tape water, River Indus and wastewater. The samples were spiked to 20 µg/mL of EBT dye and each prepared sample was used for photodegradation at optimized conditions (10 mg of ZnO catalyst, the fluorescent UV light irradiation time 30 min and pH

11). The photocatalytic activity with EBT dye varied from 85.37%, 88.25% and 82.63% in River Indus water, tape water and wastewater (Figure S9). The results revealed that degradation of EBT dye decreased in real water and wastewater, may be due to the different substances present in these water samples interfered the efficiency of degradation.

Photocatalytic Degradation Kinetic Models

The kinetic models were used for the photodegradation of EBT to know the order and speed of reaction [37]. The three kinetic models pseudo zero order, first and second order were used. The EBT dye degradation plot did not obeyed pseudo zero order with coefficient of determination (R^2) 0.8651 (Figure S10a), pseudo first order also less fitted with R^2 (0.9084) (Figure S10b), while the pseudo second-order expression better fitted with improved R^2 value (0.9628) for EBT dye degradation by ZnO (Figure S10c). According to kinetics models reaction parameters (Table S1), the rate constant decreases with increasing initial concentration and irradiation time.

Isotherm Models

The Modified Langmuir isotherm model describes the monolayer adsorption and molecules follow successive photocatalytic degradation [25, 38]. The modified Langmuir isotherm model fitted the kinetic model with linear correlation coefficient of $R^2 = 0.989$ (Figure S11a). The modified Freundlich model, is used to know the heterogeneous diffusion, and Freundlich model also fitted the kinetic model with $R^2 = 0.9548$ (Figure S11b). The Dubinin–Radushkevich (D–R) isotherm did not fitted in the kinetic model with $R^2 =$ is 0.895 (Figure S11c). Moreover, the kinetic model estimated the resemblance in the photocatalytic activity. The present work obeyed Langmuir models more as compared to Freundlich and Dubinin–Radushkevich isotherm models (Table S2).

Comparison of Degradation Efficiency with Other Nanoparticles

There are a number of nanoparticles applied for the photocatalytic degradation capability of EBT dye. These nanoparticles have different degradation capability for EBT dye (Table 3). Nevertheless these nanoparticles have disadvantages which are associated to longer time degradation process. Amongst the reported nanoparticles, the new synthesized ZnO exhibited good or comparable photocatalytic activity to many other nano materials. The present ZnO has advantages of low operating cost, eco-friendly, simplicity and excellent degradation efficiency [39–46].

Table 3 Comparison the photocatalytic degradation capacities of nanoparticles versus EBT dye

Name of nanoparticles	Dyes	Photocatalytic degradation capability	Degradation time (Minutes)	References
Titanium oxide (TiO$_2$) Nanofibers	EBT	77%	100	Zhu and Jiang [39]
Tin oxide (SnO$_2$) nanoparticles	EBT	77.00%	270	Najjar et al. [40]
NH$_2$-SiO$_2$/Cu nanocomposite	EBT	83%	50	Sarker et al. [41]
Cobalt chromite (CoCr$_2$O$_4$) nanoparticles	EBT	90%	90	Fardood et al. [42]
Cobalt oxide (Co$_3$O$_4$) nanoparticles	EBT	(39.4%)	40	Adekunle et al. [43]
CoO–CuFe$_2$O$_4$ double layered nanoparticles	EBT	99.4%	90	Ifebajo et al. [44]
Cerium oxide (CeO$_2$) nanoparticles	EBT	99.23%	120	Mishra et al. [45]
Neodymium zirconate (Nd$_2$Zr$_2$O$_7$) nanostructures	EBT	84%	50	Zinatloo-Ajabshir and Salavati-Niasari [46]
Zinc Oxide (ZnO) nanoparticles	EBT	99.63%	30	Present study

Mathematical Modeling

The mathematical modeling by adopting response surface process is increasing in field of chemistry and applied sciences.

The Response Surface (3D) Graphs

The response surface (3D) graphs were plotted to know the combined effects of factors on the degradation. The surface height of (3D) graph displays magnitude of the predicted degradation capacity of the catalyst [26, 27]. The response surface graph shows the degradation of EBT dye by ZnO as catalyst. The 3D plot (Fig. 6a) exposes the joined result of pH and concentration on degradation efficiency, the degradation decreased with increase in the concentration of EBT. The pH is important factor and influences the degradation capacity, the degradation of dye increased at higher pH level. The plot (Fig. 6b) shows joint outcome of dose of ZnO nanoparticles and pH, the degradation capacity of EBT dye increased at increasing the pH level upto 11 and ZnO dose upto 20 mg then decreased slightly. The plot (Fig. 6c) also shows joined outcome of time and pH, the degradation of EBT dye enhances with the rise in pH and increases with the irraditation time upto 30 min. The plot (Fig. 6d) shows that an increase in the concentration of EBT dye decreases the degradation % and an increase in the ZnO dose upto 20 mg increases the degradation and decreases the degradation efficiency at higher dose. The plot (Fig. 6e) displays interactive outcome of irraditation time and concentration, the degradation capacity of EBT dye decreases at higher concentration and increases at increasing the irraditation time. The plot (Fig. 6f) shows that increase in the catalyst dose increases the degradation % of dye upto 20 mg after that degradation efficiency decreases because active sites were consumed and no more dye could be degraded, and degradation efficiency of dye increased at increasing the irradiation.

Analysis of Variance (ANOVA)

The statistical importance of model was examined by analysis of variance (ANOVA). The significance of parameters may be predictable by the magnitude of F-ratio and P-values as indicated in the ANOVA (Table S3). The higher value of F and lower values of P (0.05) indicates the significance and acceptance of hypothesis [26, 47]. The F-ratios varied from 0.15 to 35.05 and P-value from 0.027 to 0.739. Variable (A, pH), (AC, pH and dose of photocatalyst) and (BD, concentration of dye and time) were significant (P=0.05). The variables (B, concentration of dye), (D, time of irradiation) and (CD, dose of photocatalyst and time of irradiation) were also significant at P=0.1(90%).

Standardized Pareto Chart

There are 2 types of pareto chart standardized and unstandardized, the unstandardized chart indicates the decreasing order of absolute levels of effects, while the standardized chart shows that each standardized effects is divided by its standard error and changed into t-statistics and then standardized effects are organized in decreasing order of their absolute levels (Fig. 7) [27]. The standardized chart shows reference line at specified important value that is usually 5% (a%), the effects which exceed this line will be measured as statistically important effects. The pareto plot is displayed in to different colors to separate the negative (inverse effect) and positive (direct effects) [48, 49]. The pareto chart effect are labeled as pH (A), concentration of dye (B), dose of catalyst (C) and irradiation time (D). The pareto plot for degradation of EBT dye showed that interaction terms pH (A), (AA), Time (D), (BD), (AC), (CC) and (BB) showed positive significant effects on degradation of EBT dye and these variable correlated to each other. The CD, DD and B concentration showed negative significant effects on degradation capacity of the catalyst (increasing the amount of
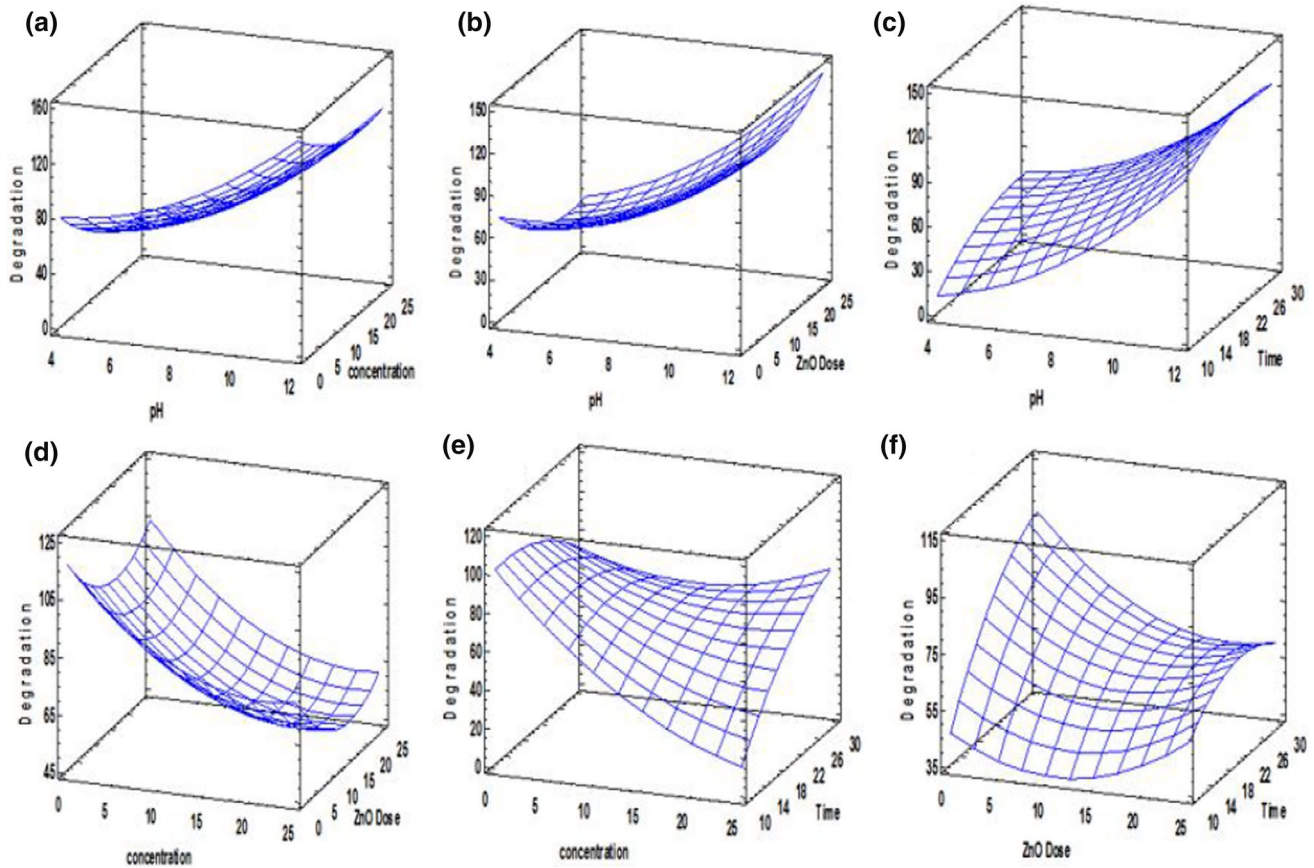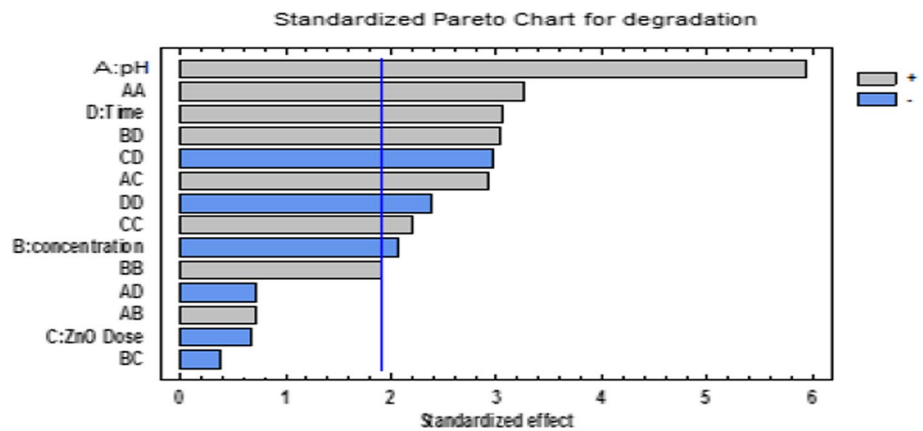
Fig. 6 Response surface (3D) graphs

Fig. 7 Standardized Pareto chart

dose and concentration decreasing the degradation efficiency of EBT dye), other variables effects did not cross the reference line therefore these variables are not significant.

Normal Probability Plot Effects

The normal probability plot is applied to know the real effects and isolated them from noise. The standardized effects points are designed from lower to higher order (positive or negative values). If the signals which are falling along the reference line or close to line will be considered as a noise and have no any effects on the response while if signals falls away from the references line will be considered as real signals and resemble to significant effects. The normal probability charts of effects for the degradation of EBT dye showed majority of points away from the reference line such as A, AA, B, BD, CC, CA, C
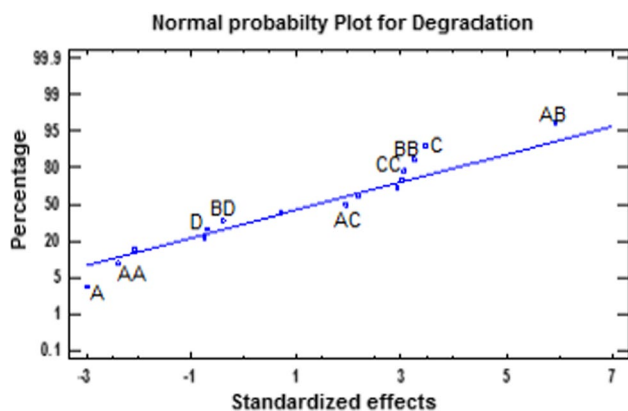
Fig. 8 Normal probability plot of effects

and AB demonstrating significant effects (negative or positive) on the degradation capacity of the catalyst (ZnO). But a few points falls along with reference line indicating as a noise and no significant effect on the response (Fig. 8) [48, 49].

Conclusion

The ZnO photocatalyst was prepared by complexation with diethyldithiocarbamate, followed by different calcination temperatures 450, 600, 750 and 900 °C. The calcination temperature 750 °C showed better photocatalytic degradation capability as compared to others. The three different sources of light were compared for the photo degradation capability of EBT dye, the fluorescent UV light showed highest photo degradation % as compared to visible and mercury light. The degradation rate of EBT dye increased, with rise of photocatalyst dosage until 20 mg dose. The basic condition pH 11 was more favorable for degradation than acidic condition and showed highest photo degradation of EBT dye. The present study obeyed pseudo second order kinetics model and isotherm model Langmuir more fitted as compared to other models. The photocatalyst ZnO indicated a comparable photodegradation of EBT dye with reported works in shorter time (30 min). The factorial design was applied to examine the important variables and their effects.

References

1. M. Hao, M. Qiu, H. Yang, B. Hu, and X. Wang (2021). Recent advances on preparation and environmental applications of MOF-derived carbons in catalysis. *Sci. Total Environ.* **760**, 143333.

2. Q. Li, Z. Chen, H. Wang, H. Yang, T. Wen, S. Wang, and X. Wang (2021). Removal of organic compounds by nanoscale zero-valent iron and its composites. *Sci. Total Environ.* **792**, 148546.

3. S. Zhang, J. Wang, Y. Zhang, J. Ma, L. Huang, S. Yu, and X. Wang (2021). Applications of water-stable metal-organic frameworks in the removal of water pollutants: a review. *Environ. Pollut.* **291**, 118076.

4. S. Yu, H. Pang, S. Huang, H. Tang, S. Wang, M. Qiu, and X. Wang (2021). Recent advances in metal-organic framework membranes for water treatment: a review. *Sci. Total Environ.* **800**, 149662.

5. Y. Zou, Y. Hu, Z. Shen, L. Yao, D. Tang, S. Zhang, and X. Wang (2022). Application of aluminosilicate clay mineral-based composites in photocatalysis. *J. Environ. Sci.* **115**, 190–214.

6. S. Chidambaram, B. Pari, N. Kasi, and S. Muthusamy (2016). ZnO/Ag heterostructures embedded in Fe_3O_4 nanoparticles for magnetically recoverable photocatalysis. *J. Alloys Compd.* **665**, 404–410.

7. D. D. Liu, Z. S. Wu, F. Tian, B. C. Ye, and Y. B. Tong (2016). Synthesis of N and La codoped TiO_2/AC photocatalyst by microwave irradiation for the photocatalytic degradation of naphthalene. *J. Alloys Compd.* **676**, 489–498.

8. Y. Liu, L. Yu, Y. Hu, C. F. Guo, F. M. Zhang, and X. W. Lou (2012). A magnetically separable photocatalyst based on nest-likeγ-Fe_2O_3/ZnO double-shelled hollow structures with enhanced photocatalytic activity. *Nanoscale* **4** (1), 183–187.

9. A. Vázquez, D. B. Hernández-Uresti, and S. Obregón (2016). Electrophoretic deposition of CdS coatings and their photocatalytic activities in the degradation of tetracycline antibiotic. *Appl. Surf. Sci.* **386**, 412–417.

10. D. Pathania, D. Gupta, H. Alaa, G. Sharma, A. Kumar, M. Naushad, et al. (2016). Photocatalytic degradation of highly toxic dyes using chitosan-g-poly (acrylamide)/ZnS in presence of solar irradiation. *J. Photochem. Photobiol. A* **329**, 61–68.

11. H. J. Lee, J. H. Kim, S. S. Park, S. S. Hong, and G. D. Lee (2015). Degradation kinetics for photocatalytic reaction of methyl orange over Al-doped ZnO nanoparticles. *J. Ind. Eng. Chem.* **25**, 199–206.

12. S. A. Ansari, M. M. Khan, M. O. Ansari, J. Lee, and M. H. Cho (2013). Biogenic synthesis, photocatalytic, and photoelectrochemical performance of Ag-ZnO nanocomposite. *J. Phys. Chem. C* **117** (51), 27023–27030.

13. S. Y. Pung, W. P. Lee, and A. Aziz (2012). Kinetic study of organic dye degradation using ZnO particles with different morphologies as a photocatalyst. *Int. J. Inorg. Chem.* **2012**, 1–9.

14. J. J. Vora, S. K. Chauhan, K. C. Parmar, S. B. Vasava, S. Sharma, and L. S. Bhutadiya (2009). Kinetic study of application of ZnO as a photocatalyst in heterogeneous medium. *J. Chem.* **6** (2), 531–536.

15. K. Byrappa, A. K. Subramani, S. Ananda, K. L. Rai, R. Dinesh, and M. Yoshimura (2006). Photocatalytic degradation of rhodamine B dye using hydrothermally synthesized ZnO. *Bull. Mater. Sci.* **29** (5), 433–438.

16. F. Barka-Bouaifel, B. Sieber, N. Bezzi, J. Benner, P. Roussel, L. Boussekey, and R. Boukherroub (2011). Synthesis and photocatalytic activity of iodine-doped ZnO nanoflowers. *J. Mater. Chem.* **21** (29), 10982–10989.

17. A. Raja, S. Ashokkumar, R. P. Marthandam, J. Jayachandiran, C. P. Khatiwada, K. Kaviyarasu, and M. Swaminathan (2018). Eco-friendly preparation of zinc oxide nanoparticles using *Tabernaemontana divaricata* and its photocatalytic and antimicrobial activity. *J. Photochem. Photobiol. B: Biol.* **181**, 53–58.

18. S. M. Taghizadeh, N. Lal, A. Ebrahiminezhad, F. Moeini, M. Seifan, Y. Ghasemi, and A. Berenjian (2020). Green and economic fabrication of zinc oxide (ZnO) nanorods as a broadband UV blocker and antimicrobial agent. *Nanomaterials* **10** (3), 530.

19. R. Vinayagam, R. Selvaraj, P. Arivalagan, and T. Varadavenkatesan (2020). Synthesis, characterization and photocatalytic dye degradation capability of *Calliandra haematocephala*-mediated zinc oxide nanoflowers. *J. Photochem. Photobiol. B: Biol.* **203**, 111760.

20. N. M. El-Shafai, M. Shukry, I. M. El-Mehasseb, M. Abdelfatah, M. S. Ramadan, A. El-Shaer, and M. El-Kemary (2020). Electrochemical property, antioxidant activities, water treatment and solar cell applications of titanium dioxide–zinc oxide hybrid nanocomposite based on graphene oxide nanosheet. *Mater. Sci. Eng.: B* **259**, 114596.

21. S. Sagadevan, S. Vennila, S. N. Suraiya Begum, Y. A. Wahab, N. A. B. Hamizi, A. R. Marlinda, and H. Algarni (2020). Influence of incorporated barium ion on the physio-chemical properties of zinc oxide nanodisks synthesized via a sonochemical process. *J. Nanosci. Nanotechnol.* **20** (9), 5452–5457.

22. S. K. Kansal, S. Sood, A. Umar, and S. K. Mehta (2013). Photocatalytic degradation of Eriochrome Black T dye using well-crystalline anatase TiO$_2$ nanoparticles. *J. Alloys Compd.* **581**, 392–397.

23. J. Labuda, M. Skatulokova, M. Nemeth, and S. Gergely (1984). Formation and stability of diethyldithiocarbamate complexes. *Chem. zvesti* **38**, 597.

24. H. Zhang, D. Liu, S. Ren, and H. Zhang (2017). Kinetic studies of direct blue photodegradation over flower-like TiO$_2$. *Res. Chem. Intermed.* **43** (3), 1529–1542.

25. M. B. Mukhlish, F. Najnin, M. M. Rahman, and M. J. Uddin (2013). Photocatalytic degradation of different dyes using TiO$_2$ with high surface area: a kinetic study. *J. Sci. Res.* **5** (2), 301–314.

26. F. Qureshi, S. Q. Memon, M. Y. Khuhawar, and T. M. Jahangir (2021). Removal of Co^{2+}, Cu^{2+} and Au^{3+} ions from contaminated wastewater by using new fluorescent and antibacterial polymer as sorbent. *Polym. Bull.* **78** (3), 1505–1533.

27. F. Qureshi, S. Q. Memon, M. Y. Khuhawar, T. M. Jahangir, and A. H. Channar (2021). Synthesis and application of fluorescent and thermally stable polyazomethine as adsorbent in the remediation of Ni (II), Cu (II) and Co (II) from wastewater systems. *J. Polym. Res.* **28** (7), 1–15.

28. A. M. Pillai, V. S. Sivasankarapillai, A. Rahdar, J. Joseph, F. Sadeghfar, K. Rajesh, and G. Z. Kyzas (2020). Green synthesis and characterization of zinc oxide nanoparticles with antibacterial and antifungal activity. *J. Mol. Struct.* **1211**, 128107.

29. M. V. Sujitha and S. Kannan (2013). Green synthesis of gold nanoparticles using Citrus fruits (*Citrus limon*, Citrus reticulata and *Citrus sinensis*) aqueous extract and its characterization. *Spectrochim. Acta Part A* **102**, 15–23.

30. A. Muthuvel, K. Adavallan, K. Balamurugan, and N. Krishnakumar (2014). Biosynthesis of gold nanoparticles using *Solanum nigrum* leaf extract and screening their free radical scavenging and antibacterial properties. *Biomed. Prev. Nutr.* **4** (2), 325–332.

31. M. Fang, X. Tan, Z. Liu, B. Hu, and X. Wang (2021). Recent progress on metal-enhanced photocatalysis: a review on the mechanism. *Research* **2021**, 1–16.

32. M. Qiu, B. Hu, Z. Chen, H. Yang, L. Zhuang, and X. Wang (2021). Challenges of organic pollutant photocatalysis by biochar-based catalysts. *Biochar* **3** (2), 117–123.

33. Z. H. Zhang, Y. Xu, X. P. Ma, F. Y. Li, D. N. Liu, Z. L. Chen, et al. (2012). Microwave degradation of methyl orange dye in aqueous solution in the presence of nano-TiO$_2$-supported activated carbon (supported-TiO$_2$/AC/MW). *J. Hazard Mater.* **209**, 271–277.

34. S. Lan, L. Liu, R. Q. Li, Z. H. Leng, and S. C. Gan (2014). Hierarchical hollow structure ZnO: synthesis, characterization, and highly efficient adsorption/photocatalysis toward Congo red. *Ind. Eng. Chem. Res.* **53** (8), 3131–3139.

35. A. Khataee, R. D. C. Soltani, A. Karimi, and S. W. Joo (2015). Sonocatalytic degradation of a textile dye over Gd-doped ZnO

36. L. Saikia, D. Bhuyan, M. Saikia, B. Malakar, D. K. Dutta, and P. Sengupta (2015). Photocatalytic performance of ZnO nanomaterials for self sensitized degradation of malachite green dye under solar light. *Appl. Catal. A Gen.* **490**, 42–49.

37. I. Ali, O. M. Alharbi, Z. A. Alothman, and A. Y. Badjah (2018). Kinetics, thermodynamics, and modeling of amido black dye photodegradation in water using Co/TiO$_2$ nanoparticles. *Photochem. Photobiol* **94** (5), 935–941.

38. F. Moeinpour, A. Alimoradi, and M. Kazemi (2014). Efficient removal of Eriochrome black-T from aqueous solution using NiFe$_2$O$_4$ magnetic nanoparticles. *J. Environ. Health Sci. Eng.* **12** (1), 1–7.

39. J. Zhu and Z. Jiang (2021). Electrochemical photocatalytic degradation of eriochrome black T dye using synthesized TiO$_2$@ CNTs nanofibers. *Int. J. Electrochem. Sci.* **16**, 210318.

40. M. Z. Sarker, M. M. Rahman, H. Minami, T. Suzuki, M. K. Hossain, and H. Ahmad (2021). Mesoporous amine functionalized SiO$_2$ supported Cu nanocatalyst and a kinetic-mechanistic degradation study of azo dyes. *Coll. Surf. A* **617**, 126403.

41. M. Najjar, H. A. Hosseini, A. Masoudi, Z. Sabouri, A. Mostafapour, M. Khatami, and M. Darroudi (2021). Green chemical approach for the synthesis of SnO$_2$ nanoparticles and its application in photocatalytic degradation of Eriochrome Black T dye. *Optik* **242**, 167152.

42. S. T. Fardood, R. Forootan, F. Moradnia, Z. Afshari, and A. Ramazani (2020). Green synthesis, characterization, and photocatalytic activity of cobalt chromite spinel nanoparticles. *Mater. Res. Express* **7** (1), 015086.

43. A. S. Adekunle, J. A. Oyekunle, L. M. Durosinmi, O. S. Oluwafemi, D. S. Olayanju, A. S. Akinola, and T. A. Ajayeoba (2020). Potential of cobalt and cobalt oxide nanoparticles as nanocatalyst towards dyes degradation in wastewater. *Nano-Struct. Nano-Objects* **21**, 100405.

44. A. O. Ifebajo, A. A. Oladipo, and M. Gazi (2020). Sun-light driven enhanced azo dye decontamination from aqueous solution by CoO– CuFe. *Desalin. Water Treat.* **177** (2020), 423–430.

45. S. Mishra, S. Soren, A. K. Debnath, D. K. Aswal, N. Das, and P. Parhi (2018). Rapid microwave–Hydrothermal synthesis of CeO$_2$ nanoparticles for simultaneous adsorption/photodegradation of organic dyes under visible light. *Optik* **169**, 125–136.

46. S. Zinatloo-Ajabshir and M. Salavati-Niasari (2017). Photo-catalytic degradation of erythrosine and eriochrome black T dyes using Nd$_2$Zr$_2$O$_7$ nanostructures prepared by a modified Pechini approach. *Sep. Purif. Technol.* **179**, 77–85.

47. S. H. Hasan, P. Srivastava, and M. Talat (2009). Biosorption of Pb (II) from water using biomass of *Aeromonas hydrophila*: central composite design for optimization of process variables. *J. Hazard. Mater.* **168** (2–3), 1155–1162.

48. M. Mouelhi, I. Marzouk, and B. Hamrouni (2016). Optimization studies for water defluoridation by adsorption: application of a design of experiments. *Desalin. Water Treat.* **57** (21), 9889–9899.

49. A. Baskar and P. S. Shabudeen (2015). Factorial design of experiment model enables to optimize the variables in wastewater decolorization process by using areca husk activated carbon fibre. *J. Chem. Pharm. Res.* **7** (4), 1500–1511.